Closed-Form Formulas for Hyperbolically Tapered Rotating Disks Made of Traditional Materials under Combined Thermal and Mechanical Loads

Vebil Yıldırım

Department of Mechanical Engineering, Faculty of Engineering, University of Çukurova, Adana, Turkey
E-mail address: vebil@cu.edu.tr

ORCID numbers of authors:
0000-0001-9955-8423

Abstract

Using the true temperature distribution along the radial coordinate, closed-form formulas are offered for readers to study the thermo-mechanical behavior of variable thickness disks having both convergent and divergent hyperbolic thickness profiles made of conventional materials. Internal and external pressures, centrifugal forces and thermal loads due to the differences in prescribed surface temperatures are all considered with three boundary conditions: free-free (a circular annulus), fixed-free (a disk mounted on a rotating shaft at the inner surface), and fixed-fixed (a disk mounted on a rotating shaft at the inner surface and cased at the outer surface) boundary conditions. A parametric study is also conducted in almost real working environment in which the outer surface of the disk has considerably higher temperature rather than the inner surface. The thermomechanical linear elastic response of a hyperbolic mounted rotating disk subjected to the external pressure induced by blades is originally handled by those proposed formulas.

Keywords: Variable thickness disk, nonuniform rotating disk, closed-form elasticity solution, exact solution, analytical solution, thermomechanical, thermal analysis.

1. Introduction

As a rotating machinery element, rotating disks may operate as a circular annulus or as a disk attaching a rotating shaft at its center. A rigid casing may exist at the outer surface of such a disk. Their thickness may vary along the radial direction linearly, hyperbolically, parabolically, exponentially or so on and so forth. It may be made of any kind of traditional or advanced materials. Rotating disks may act in high temperature environments like turbine rotors, flywheels and gears and may be subjected to simultaneously external pressures due to the existence of the blades. In such cases, the thermo-mechanical analyses come into prominence in the design of such structures. It is obvious that the existence of closed-form formulas that can be directly used in the design stage in relation to the subject matter is to be of great convenience for engineers.

Thermal-related analyses of uniform disks made of an isotropic and homogeneous materials have paid much attention than disks having varying section properties and made of advanced

composite materials [1-10]. From those, Güven and Altay [1] investigated the elastic–plastic stress distribution of a solid disk due to nonuniform heat source under external pressure. Kulkarni and Deshmukh [4] addressed the thermal stresses in a thick annular disk under steady temperature field. Nejad and Afshin [6] offered an analytical solution of transient thermoelastic behaviors of rotating pressurized disks subjected to arbitrary boundary and initial conditions. Kaur et al. [8] observed that thermal effect in the disk increase the value of circumferential stress at the internal surface and radial stresses at the external surface for compressible as compare to incompressible material. Based on a variational principle considering the radial displacement field as unknown, Nayak and Saha [9] evaluated the influence of thermo-mechanical loading on stresses and deformation states in a rotating disk with varying thicknesses. They considered different disk geometries as well as temperature distribution profiles to calculate the limit angular speed of the disks under thermo-mechanical loading. Yıldırım [10] offered a consistent and an all-in-one analytical study for the determination of heat-induced, pressure-induced, and centrifugal force-induced axisymmetric exact deformation and stresses in a thick-walled spherical vessel, a cylindrical vessel, and a uniform disk at specified constant surface temperatures and at a constant angular velocity. Yıldırım [10] included both the inner and outer pressures in the formulation of annular structures made of an isotropic and homogeneous linear elastic material. For disks, three different boundary conditions were taken into account to consider mechanical engineering applications in the study [10].

Thermal-related analyses of uniform disks made of anisotropic materials [11-19] and functionally graded materials [20-28] are other investigation themes. Unfortunately, the number of studies on the thermal/thermal related analysis of variable thickness disks made of either functionally graded (FG) materials [29-42] or traditional materials [43-46] are not enough. In those studies, a variable-thickness disk is generally considered as a combination of multi-layered uniform disks [29, 30-32, 34, 36, 40]. For example, Chiba [29] assumed the annular disk is to be a multilayered one with stepwise thickness variation, where each layer is assumed to have constant deterministic material properties. Bayat et al. [30] considered a rotating FG disk with either parabolic or hyperbolic thickness under a steady temperature field. The disk was assumed to be composed of sub-disks of uniform thicknesses. In another study, Bayat et al. [31] analyzed the thermoelastic bending of FGM rotating disks based on the first order shear deformation theory. Bayat et al. [32] studied on a thermo elastic analysis for axisymmetric rotating disks made of temperature-dependent power-law FG material with variable thickness. It was assumed in Ref. [32] that the temperature field is to be uniformly distributed over the disk surface and varied in the radial direction. Bayat et al. [32] presented semi-analytical solutions for the displacement field for solid/annular disks under free-free and fixed-free boundary conditions. Bayat et al. [33] also offered exact elastic solutions for axisymmetric variable-thickness hollow rotating disks with heat source made of functionally power-law-graded (FG) materials under free-free and fixed-free boundary conditions. They showed that the temperature distribution in a hyperbolic disk is the smallest compared with other thickness profiles. A hyperbolic-convergent FG disk has smaller stresses because of thermal load compared with the uniform disk. Nie and Batra [35] studied axisymmetric stresses in a rotating disk made of a rubber-like material that was modeled as isotropic, linear thermoelastic, and incompressible. Damircheli and Azadi [36] carried out thermal and mechanical stress analyses of a rotating disk having either parabolically or hyperbolically varying thicknesses made of functionally graded material by using finite element method (FEM). By utilizing a 2D plane stress analysis and assuming a power form temperature distribution of over the disk with the higher temperature at the outer surface, Hassani et al. [37] obtained stress and strains of rotating disks with non-uniform thickness and material properties subjected to thermo-elastic loading

under different boundary conditions. They used semi-exact methods of Liao's homotopy analysis method (HAM), Adomian's decomposition method and He's variational iteration method (VIM). Hassani et al. [37] compared the results of those three methods with Runge–Kutta's solutions. Tütüncü and Temel [38] studied numerically the thermoelastic analysis of FG rotating disks of variable thickness. Golmakani [39] scrutinized large deflection thermoelastic analysis of FG solid and hollow rotating axisymmetric disk with uniform and variable thickness subjected to thermo-mechanical loading. Kurşun and Topçu [40] handled the elastic stress analysis of a hollow disk with variable thickness made of FG materials under linearly increasing temperature distribution. Mahdavi et al. [41] worked on the thermoplastic analysis of FG rotating hyperbolic disks by dividing the domain into some finite sub-domains in the radial direction, in which the properties were assumed to be constant. Recently, Jabbari et. al. [42] presented a thermoelastic analysis of rotating disks with different thickness profiles made of power-graded and exponential-graded materials subjected to internal pressure. They verified the results with finite element method.

As stated above, there are also relatively less study on the thermal-related analyses of isotropic and homogeneous disks with varying thickness. By using hyper-geometric differential equation in terms of radial displacement, Vivio and Vullo [43] and Vullo and Vivio [44] introduced an analytical procedure for evaluation of elastic stresses and strains in rotating conical disks and in non-linear variable thickness rotating disks made of an isotropic and homogeneous material, either solid or annular, subjected to thermal loads. In the presence of the linear thermal gradient, Garg et al. [45] analyzed the steady state creep in a rotating disk having linearly varying thickness and made of composite containing silicon carbide particles (SiC) in a matrix of pure aluminium. Çetin et al. [46] studied analytically an elastic stress analysis of annular isotropic and homogeneous bi-material hyperbolic disks subjected to the mechanical and thermo-mechanical loads.

As can be seen from the literature survey mentioned above, the realm of the thermal-related analyses of such disks having varying thicknesses needs further works.

In the present study, the exact distribution of the temperature along the radial coordinate in a hyperbolic disk is, first, obtained analytically based on the solution of Fourier heat-conduction differential equation under thermal boundary conditions defined by specified surface temperatures. This closed-form solution for temperature distribution is, then, substitute in the Navier equation obtained for the elasto-static response of such disks. Finally, Navier equations containing thermal effects are solved by applying mechanical boundary conditions. In the solution process of both the heat conduction and Navier equations, both of which are in the form of a second order differential equation with constant coefficients, a well-known Euler-Cauchi technique is employed [47]. Those formulas are compared with those available in the open literature.

2. Formulation of the Thermal Behavior of the Disk

An accurate solution of the temperature field in the structure is a crucial first step to study the thermal-related analyses in an appropriate manner. The rate of the heat flux, $\boldsymbol{q}$, in a solid object is proportional to the temperature gradient, $\boldsymbol{\nabla}T$. The Fourier law governing the heat transfer by conduction is

$$\boldsymbol{q} = -k\boldsymbol{\nabla}T = -k\, grad(T) \tag{1}$$

where k is the thermal conductivity. Temperature gradient is given in cylindrical coordinates, (r,θ,z), by

$$\nabla T = grad(T) = \frac{\partial T}{\partial r}\boldsymbol{e}_r + \frac{1}{r}\frac{\partial T}{\partial \theta}\boldsymbol{e}_\theta + \frac{\partial T}{\partial z}\boldsymbol{e}_z \tag{2}$$

where ($\boldsymbol{e}_r, \boldsymbol{e}_\theta, \boldsymbol{e}_z$) are the unit vectors in cylindrical coordinates, r is the radial coordinate, θ is the circumferential coordinate. By using the first law of thermodynamics, Fourier heat conduction equation may be written as follows.

$$\rho c_p \frac{\partial T}{\partial t} + div(\boldsymbol{q}) = \dot{q}_{gen} \tag{3}$$

where ρ is the density, and c_p is the specific heat capacity, $\dot{q}_{gen}$ is the heat generation per unit volume. Using Eq. (1) the following may be written for the divergence of the heat flux as

$$div(\boldsymbol{q}) = \nabla.\boldsymbol{q} = -k(\nabla.\nabla T) = -k\Delta T = -k\nabla^2 T \tag{4}$$

By assuming that there is no heat generation in the structure, $\dot{q}_{gen} = 0$, and the steady state case ($\partial T/\partial t = 0$) exists, substitution of Eq. (4) into the heat conduction equation (3) gives the Laplacian of the temperature that is the divergence of the gradient of the temperature as follows

$$k\nabla^2 T = k\left(\frac{1}{r}\frac{\partial}{\partial r}\left(r\frac{\partial T}{\partial r}\right) + \frac{1}{r^2}\frac{\partial^2 T}{\partial \theta^2} + \frac{\partial^2 T}{\partial z^2}\right) = 0 \tag{5}$$

This is a differential equation governing steady state 3-D temperature distribution for both cylinders and discs having uniform thickness and constant thermal conductivity without heat generation. As observed from this equation and Eq. (1), both the temperature field and heat flux distribution will be the same for both cylinders and disks with uniform thickness. However, a disk with variable thickness offers different temperature and heat flux profiles than hollow cylinders and uniform disks even for a constant thermal conductivity. For axisymmetric problems (derivatives with respect to θ and z are all zero) of a variable thickness disk, Eq. (5) takes the form of

$$\frac{k}{rh(r)}\frac{d}{dr}\left(rh(r)\frac{dT(r)}{dr}\right) = 0 \tag{6}$$

It can be concluded from the above that the temperature field is to be the same for all materials exhibiting both isotropy and homogeneity properties as in the traditional materials although the material type is to be of important in the heat flux calculations. For any thickness profile, $h(r)$, defined by a differentiable function, Eq. (6) may also be written as

$$\frac{d^2 T(r)}{dr^2} + \left(\frac{1}{r} + \frac{\frac{dh(r)}{dr}}{h(r)}\right)\frac{dT(r)}{dr} = 0 \tag{7}$$

Now, consider a hyperbolic disc profile defined by

$$h(r) = h_o\left(\frac{r}{a}\right)^m \tag{8}$$

where a denotes the inner radius of the disk, m is the profile parameter, and h_o is the reference thickness (Fig. 1). While $m > 0$ defines divergent hyperbolic profiles, $m < 0$ identifies convergent ones. Uniform thickness disks are characterized by $m = 0$ (Fig. 1).

Convergent disc (m<0)

Divergent disc (m>0)
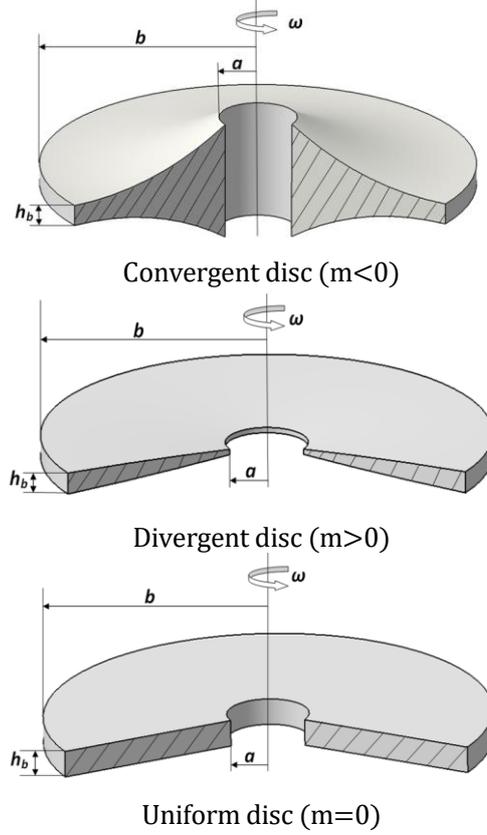
Uniform disc (m=0)

Fig. 1. 3-D view of convergent/divergent hyperbolic and uniform disc profiles

Substitution of Eq. (8) into Eq. (7) gives

$$\frac{d^2 T(r)}{dr^2} + \frac{(1+m)}{r}\frac{dT(r)}{dr} = 0 \tag{9}$$

This is an Euler-Cauchy type differential equation with constant coefficients. Solution of Eq. (9) is given by [47]

$$T(r) = C_1 r^{\mu_1} + C_2 r^{\mu_2} \tag{10}$$

where μ_1 and μ_2 are the distinct characteristic real roots of the differential equation while C_1 and C_2 are integration constants. All types of thermal boundary conditions such as Dirichlet's, Neumann's, Robin's and mixed boundary conditions may be applied to determine the integration constants of the physical problem. In the present study the first kind boundary conditions (Dirichlet) are to be considered.

$$T(a) = T_a, \quad T(b) = T_b \tag{11}$$

In the above, T_a and T_b are the inner surface and outer surface temperatures, respectively. Considering Eq. (10) together with Eq. (11), a closed form solution for the temperature distribution in a hyperbolic disk along the radial coordinate is obtained as follows

$$T(r)^{(hyperbolic)} = r^{-m}\left(\frac{a^m b^m (T_b - T_a)}{a^m - b^m}\right) + \left(\frac{a^m T_a - b^m T_b}{a^m - b^m}\right) = r^{-m}\psi_1 + \psi_2 \tag{12}$$

As seen from Eq. (12), temperature distribution in a hyperbolic disk becomes indefinite when the uniform thickness is concerned with $m = 0$. In this case either a numerical value very close to zero but not exactly equal to zero such as $m = 0.000000000001$ may be used directly in Eq. (12) or Eq. (9) is resolved for $m = 0$ under the same boundary conditions [11] to get the following

$$T(r)^{(uniform)} = \left(\frac{lna T_b - T_a lnb}{lna - lnb}\right) + \left(\frac{T_a - T_b}{lna - lnb}\right)lnr = \emptyset_2 + \emptyset_1 lnr \tag{13}$$

3. Formulation of the Thermo-mechanical Behavior of the Disk

Under small deformations and a state of axisymmetric plane stress assumptions for thin plates, field equations of a variable thickness rotating disk made of a traditional material in polar coordinates (r, θ) are reduced to

$$\varepsilon_r(r) = \frac{du_r(r)}{r}, \quad \varepsilon_\theta(r) = \frac{u_r(r)}{r} \tag{14a}$$

$$\sigma_r(r) = \frac{E}{(1 - v^2)}\varepsilon_r(r) + \frac{Ev}{(1 - v^2)}\varepsilon_\theta(r) - \frac{E(1 + v)}{(1 - v^2)}\alpha T \tag{14b}$$

$$\sigma_\theta(r) = \frac{Ev}{(1 - v^2)}\varepsilon_r(r) + \frac{E}{(1 - v^2)}\varepsilon_\theta(r) - \frac{E(1 + v)}{(1 - v^2)}\alpha T \tag{14c}$$

$$\frac{d}{dr}\left(rh(r)\sigma_r(r)\right) - h(r)\sigma_\theta(r) = -\rho h(r)\omega^2 r^2 \tag{14d}$$

where $u_r(r)$ is the radial displacement, $\varepsilon_r(r)$ and $\varepsilon_\theta(r)$ are the radial and circumferential strains, respectively; $\sigma_r(r)$ is the radial stress, $\sigma_\theta(r)$ is the hoop stress, ω is a constant angular velocity, ρ is the material density, E is Young's modulus, α is is the coefficient of expansion of the disc material and v is Poisson's ratio.

Equations (14a) are called the strain-displacement relations, Eqs. (14b) and (14c) are referred to as linear elastic stress-strain relations, and finally Eq. (14d) is the equilibrium equation under the centrifugal forces. Navier equation which is in the form of a second order differential equation with variable coefficients is derived from the field equations given in Eq. (14) as follows

$$\frac{d^2 u_r(r)}{dr^2} + \left(\frac{1}{r} + \frac{\frac{dh(r)}{dr}}{h(r)}\right)\frac{du_r(r)}{dr}$$

$$+ \left(-\frac{1}{r^2} + \frac{v}{r}\frac{\frac{dh(r)}{dr}}{h(r)}\right)u_r(r) = -\frac{(1 - v^2)}{E}\rho\omega^2 r - \alpha(1 + v)\frac{dT(r)}{dr} \tag{15}$$

By using Eqs. (8) and (12), Eq. (15) may be written for a hyperbolic disk as follows

$$\frac{d^2u_r(r)}{dr^2} + \frac{(1+m)}{r}\frac{du_r(r)}{dr} + \frac{(-1+mv)}{r^2}u_r(\text{r}) = -\frac{(1-v^2)}{E}\rho\omega^2 r + r^{-(1+m)}\Delta \tag{16}$$

where

$$\Delta = -m\alpha(1+v)\psi_1 \tag{17}$$

For a uniform thickness disk, Eq. (15) is rewritten by considering Eq. (13) as follows [10]

$$\frac{d^2u_r(r)}{dr^2} + \frac{1}{r}\frac{du_r(r)}{dr} - \frac{1}{r^2}u_r(\text{r}) = -\frac{(1-v^2)}{E}\rho\omega^2 r + \alpha(1+v)\frac{\emptyset_1}{r} \tag{18}$$

4. Closed-form Solutions of Navier Equations

The closed-form solutions of both Eqs. (16) and (18) under each mechanical boundary conditions presented in Table 1 are to be given in this section. Those formulas may be used by recalling that the superposition principle holds.

$$u_r(r)^{(Thermomechanical)} = u_r(r)^{(Pressure)} + u_r(r)^{(Rotation)} + u_r(r)^{(Thermal)}$$

$$\sigma_r(r)^{(Thermomechanical)} = \sigma_r(r)^{(Pressure)} + \sigma_r(r)^{(Rotation)} + \sigma_r(r)^{(Thermal)} \tag{19}$$

$$\sigma_\theta(r)^{(Thermomechanical)} = \sigma_\theta(r)^{(Pressure)} + \sigma_\theta(r)^{(Rotation)} + \sigma_\theta(r)^{(Thermal)}$$

The equivalent von-Mises stresses by an axisymmetric plane stress assumption may be computed by

$$\tag{20}$$

$$\sigma_{eq}(r)^{(Thermomechanical)} = \left(\sqrt{\sigma_r(r)^2 + \sigma_\theta(r)^2 - \sigma_r(r)\sigma_\theta(r)}\right)^{(Thermomechanical)}$$

Table 1. Mechanical boundary conditions

Free-Free (circular annulus)	Fixed-Free (mounted disk)	Fixed-Fixed (mounted and cased disk)
$\sigma_r(a) = -p_a$ $\sigma_r(b) = -p_b$	$u_r(a) = 0$ $\sigma_r(b) = -p_b$	$u_r(a) = 0$ $u_r(b) = 0$
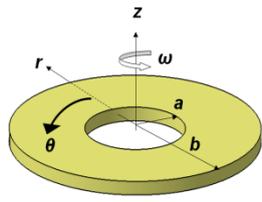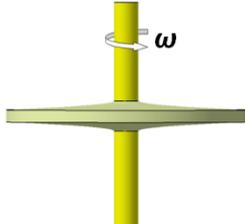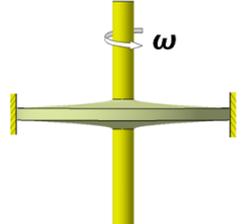
4.1. Under Mechanical Pressure Loads

Elastic fields in a hyperbolic disk subjected to both the internal and external pressures ($\omega = 0$, $\alpha = 0$) are found under free-free conditions as

$$u_r(r)_{(Free-Free)}^{(Pressure)} = \left\{ -\frac{2(v^2-1)p_a a^{\frac{1}{2}(m+\Phi+2)} r^{\frac{1}{2}(-m-\Phi)} \begin{pmatrix} b^\Phi(m-2v-\Phi) \\ -r^\Phi(m-2v+\Phi) \end{pmatrix}}{E(a^\Phi - b^\Phi)(m-2v+\Phi)(-m+2v+\Phi)} \right\}$$

$$+ \left\{ -\frac{2(v^2-1)p_b b^{\frac{1}{2}(m+\Phi+2)} r^{\frac{1}{2}(-m-\Phi)} \begin{pmatrix} a^\Phi(-m+2v+\Phi) \\ +r^\Phi(m-2v+\Phi) \end{pmatrix}}{E(a^\Phi - b^\Phi)(m-2v+\Phi)(-m+2v+\Phi)} \right\}$$

(21a)

$$\sigma_r(r)_{(Free-Free)}^{(Pressure)} = \left\{ \frac{p_a a^{\frac{1}{2}(m+\Phi+2)} (b^\Phi - r^\Phi) r^{\frac{1}{2}(-m-\Phi-2)}}{a^\Phi - b^\Phi} \right\}$$

$$+ \left\{ \frac{p_b(a^\Phi - r^\Phi) b^{\frac{1}{2}(m+\Phi+2)} r^{\frac{1}{2}(-m-\Phi-2)}}{b^\Phi - a^\Phi} \right\}$$

(21b)

$$\sigma_\theta(r)_{(Free-Free)}^{(Pressure)} = \left\{ \frac{p_a a^{\frac{1}{2}(m+\Phi+2)} r^{\frac{1}{2}(-m-\Phi-2)} \begin{pmatrix} b^\Phi(m-2v-\Phi)(v(m+\Phi)-2) \\ +r^\Phi(m-2v+\Phi)(-mv+v\Phi+2) \end{pmatrix}}{(a^\Phi - b^\Phi)(m-2v-\Phi)(m-2v+\Phi)} \right\}$$

$$+ \left\{ \frac{p_b b^{\frac{1}{2}(m+\Phi+2)} r^{\frac{1}{2}(-m-\Phi-2)} \begin{pmatrix} a^\Phi(m-2v-\Phi)(v(m+\Phi)-2) \\ +r^\Phi(m-2v+\Phi)(-mv+v\Phi+2) \end{pmatrix}}{(a^\Phi - b^\Phi)(m-2v+\Phi)(-m+2v+\Phi)} \right\}$$

(21c)

under fixed-free conditions as

$$u_r(r)_{(Fixed-Free)}^{(External\ Pressure)} = \left\{ -\frac{2(v^2-1)p_b(a^\Phi - r^\Phi) b^{\frac{1}{2}(m+\Phi+2)} r^{\frac{1}{2}(-m-\Phi)}}{E(a^\Phi(m-2v+\Phi)+b^\Phi(-m+2v+\Phi))} \right\}$$

(22a)

$$\sigma_r(r)_{(Fixed-Free)}^{(External\ Pressure)} = \left\{ -\frac{p_b b^{\frac{1}{2}(m+\Phi+2)} r^{\frac{1}{2}(-m-\Phi-2)} \begin{pmatrix} a^\Phi(m-2v+\Phi) \\ +r^\Phi(-m+2v+\Phi) \end{pmatrix}}{a^\Phi(m-2v+\Phi)+b^\Phi(-m+2v+\Phi)} \right\}$$

(22b)

$$\sigma_\theta(r)_{(Fixed-Free)}^{(External\ Pressure)} = \left\{ -\frac{p_b b^{\frac{1}{2}(m+\Phi+2)} r^{\frac{1}{2}(-m-\Phi-2)} \begin{pmatrix} a^\Phi(v(m+\Phi)-2) \\ +r^\Phi(-mv+v\Phi+2) \end{pmatrix}}{a^\Phi(m-2v+\Phi)+b^\Phi(-m+2v+\Phi)} \right\}$$

(22c)

In Eqs. (21) and (22)

$$\Phi = \sqrt{4 + m^2 - 4mv}$$

(23)

Equation (21) is a special application of formulas derived for functionally graded disks in Ref. [48]. Homogeneous solutions of Eq. (18) for free-free disks are ($\omega = 0$, $\alpha = 0$)

$$u_r(r)_{(Free-Free/Uniform\,Thickness)}^{(Pressure)}$$
$$= \left\{-\frac{a^2 p_a(b^2(v+1)-(v-1)r^2)}{Er(a^2-b^2)}\right\} + \left\{\frac{b^2 p_b(a^2(v+1)-(v-1)r^2)}{Er(a^2-b^2)}\right\} \quad (24a)$$

$$\sigma_r(r)_{(Free-Free/Uniform\,Thickness)}^{(Pressure)} = \left\{\frac{a^2 p_a(b^2-r^2)}{r^2(a^2-b^2)}\right\} + \left\{\frac{b^2(a^2-r^2)p_b}{r^2(b^2-a^2)}\right\} \quad (24b)$$

$$\sigma_\theta(r)_{(Free-Free/Uniform\,Thickness)}^{(Pressure)} = -\left\{\frac{a^2 p_a(b^2+r^2)}{r^2(a^2-b^2)}\right\} + \left\{\frac{b^2(a^2+r^2)p_b}{r^2(a^2-b^2)}\right\} \quad (24c)$$

Closed-form solutions in Eq. (24) overlaps with Roark's formulas [49]. For a uniform mounted disk subjected to the only external pressure, solutions become

$$u_r(r)_{(Fixed-Free/Uniform\,Thickness)}^{(External\,Pressure)} = \left\{\frac{b^2(v^2-1)p_b(a-r)(a+r)}{Er(a^2(v-1)-b^2(v+1))}\right\} \quad (25a)$$

$$\sigma_r(r)_{(Fixed-Free/Uniform\,Thickness)}^{(External\,Pressure)} = \left\{\frac{b^2 p_b((v+1)r^2-a^2(v-1))}{r^2(a^2(v-1)-b^2(v+1))}\right\} \quad (25b)$$

$$\sigma_\theta(r)_{(Fixed-Free/Uniform\,Thickness)}^{(External\,Pressure)} = \left\{\frac{b^2 p_b(a^2(v-1)+(v+1)r^2)}{r^2(a^2(v-1)-b^2(v+1))}\right\} \quad (25c)$$

To the best of the author's knowledge, Eqs. (22) and (25) are offered for the first time in the present study. These equations may be directly used to better simulate aero-disks subjected to blade pressures.

4.2. Under Mechanical Centrifugal Forces

If a disk is assumed to only rotate about an axis passing through its centroid at a constant angular velocity, the general solution of Eq. (16) is to be

$$u_r(r)^{(Rotation)} = r^{\frac{1}{2}(-m-\Phi)}(B_1 + B_2 r^\Phi) + r^3\Omega \quad (26a)$$

$$\sigma_r(r)^{(Rotation)} = \frac{1}{2}\left(\frac{E}{1-v^2}\right)r^{\frac{1}{2}(-2-m-\Phi)}\begin{pmatrix} -B_1(m-2v+\Phi) \\ +B_2 r^\Phi(-m+2v+\Phi) \\ +2r^{\frac{1}{2}(6+m+\Phi)}(3+v)\Omega \end{pmatrix} \quad (26b)$$

$$\sigma_\theta(r)^{(Rotation)} = \frac{1}{2}\left(\frac{E}{1-v^2}\right)r^{\frac{1}{2}(-2-m-\Phi)}\begin{pmatrix} B_2 r^\Phi(2-mv+v\Phi) \\ -B_1(-2+v(m+\Phi)) \\ +2r^{\frac{1}{2}(6+m+\Phi)}(1+3v)\Omega \end{pmatrix} \quad (26c)$$

where

$$\Phi = \sqrt{4+m^2-4mv}, \qquad \Omega = \frac{(-1+v^2)\rho\omega^2}{E(8+m(3+v))} \quad (27)$$

81

and

$$B_1^{(Free-Free)} = \frac{2(\nu+3)\Omega a^{\Phi} b^{\frac{1}{2}(m+\Phi+6)} - 2(\nu+3)\Omega b^{\Phi} a^{\frac{1}{2}(m+\Phi+6)}}{(a^{\Phi} - b^{\Phi})(m - 2\nu + \Phi)}$$

(28a)

$$B_2^{(Free-Free)} = \frac{2(\nu+3)\Omega \left(a^{\frac{1}{2}(m+\Phi+6)} - b^{\frac{1}{2}(m+\Phi+6)} \right)}{(a^{\Phi} - b^{\Phi})(m - 2\nu - \Phi)}$$

$$B_1^{(Fixed-Free)} = \frac{\Omega b^{\Phi} a^{\frac{1}{2}(m+\Phi+6)}(m - 2\nu - \Phi) + 2(\nu+3)\Omega a^{\Phi} b^{\frac{1}{2}(m+\Phi+6)}}{a^{\Phi}(m - 2\nu + \Phi) + b^{\Phi}(-m + 2\nu + \Phi)}$$

(28b)

$$B_2^{(Fixed-Free)} = -\frac{\Omega \left(a^{\frac{1}{2}(m+\Phi+6)}(m - 2\nu + \Phi) + 2(\nu+3)b^{\frac{1}{2}(m+\Phi+6)} \right)}{a^{\Phi}(m - 2\nu + \Phi) + b^{\Phi}(-m + 2\nu + \Phi)}$$

$$B_1^{(Fixed-Fixed)} = \frac{\Omega \left(b^{\Phi} a^{\frac{1}{2}(m+\Phi+6)} - a^{\Phi} b^{\frac{1}{2}(m+\Phi+6)} \right)}{a^{\Phi} - b^{\Phi}}$$

(28c)

$$B_2^{(Fixed-Fixed)} = -\frac{\Omega \left(a^{\frac{1}{2}(m+\Phi+6)} - b^{\frac{1}{2}(m+\Phi+6)} \right)}{a^{\Phi} - b^{\Phi}}$$

Solutions (26) is a special case of the formulas in Refs. [50-51]. If a uniform rotating disk is concerned, solutions turn to be [10, 49]

$$u_r(r)_{(Free-Free/Uniform)}^{(Rotation)}$$
$$= \frac{\rho\omega^2 \left(a^2(\nu+3)(b^2(\nu+1) - (\nu-1)r^2) - (\nu-1)r^2(b^2(\nu+3) - (\nu+1)r^2) \right)}{8Er}$$

(29a)

$$\sigma_r(r)_{(Free-Free/Uniform)}^{(Rotation)} = \frac{(\nu+3)\rho\omega^2(a^2 - r^2)(r^2 - b^2)}{8r^2}$$

(29b)

$$\sigma_\theta(r)_{(Free-Free/Uniform)}^{(Rotation)} = \frac{\rho\omega^2 \left(a^2(\nu+3)(b^2 + r^2) + r^2(b^2(\nu+3) - (3\nu+1)r^2) \right)}{8r^2}$$

(29c)

and

$$u_r(r)_{(Fixed-Free/Uniform)}^{(Rotation)}$$
$$= \frac{(\nu^2-1)\rho\omega^2(a-r)(a+r)\begin{pmatrix} a^2(b^2(\nu+1) - (\nu-1)r^2) \\ +b^2((\nu+1)r^2 - b^2(\nu+3)) \end{pmatrix}}{8Er(a^2(\nu-1) - b^2(\nu+1))}$$

(30a)

$$\sigma_r(r)_{(Fixed-Free/Uniform)}^{(Rotation)} = \frac{\rho\omega^2(r^2 - b^2)\begin{pmatrix} a^4(\nu^2-1) \\ -a^2(\nu-1)(\nu+3)(b^2 + r^2) \\ +b^2(\nu+1)(\nu+3)r^2 \end{pmatrix}}{8r^2(a^2(\nu-1) - b^2(\nu+1))}$$

(30b)

$$\sigma_\theta(r)_{(Fixed-Free/Uniform)}^{(Rotation)} = \frac{\rho\omega^2 \begin{pmatrix} a^4(v^2-1)(b^2+r^2) \\ -a^2(v-1)(b^4(v+3)+(3v+1)r^4) \\ -b^2(v+1)r^2(b^2(v+3)-(3v+1)r^2) \end{pmatrix}}{8r^2(a^2(v-1)-b^2(v+1))} \tag{30c}$$

and

$$u_r(r)_{(Fixed-Fixed/Uniform\ Thickness)}^{(Rotation)} = \frac{(v^2-1)\rho\omega^2(r^2-a^2)(r^2-b^2)}{8Er} \tag{31a}$$

$$\sigma_r(r)_{(Fixed-Fixed/Uniform\ Thickness)}^{(Rotation)} = \frac{\rho\omega^2 \begin{pmatrix} a^2((v+1)r^2-b^2(v-1)) \\ +r^2(b^2(v+1)-(v+3)r^2) \end{pmatrix}}{8r^2} \tag{31b}$$

$$\sigma_\theta(r)_{(Fixed-Fixed/Uniform\ Thickness)}^{(Rotation)} = \frac{\rho\omega^2 \begin{pmatrix} a^2(b^2(v-1)+(v+1)r^2) \\ +r^2(b^2(v+1)-(3v+1)r^2) \end{pmatrix}}{8r^2} \tag{31c}$$

4.3. Under Thermal Loads

If a disk is assumed to be subjected only thermal loads induced by temperature differences at the inner and outer surfaces, the homogeneous plus particular solutions of Eq. (16) are to be

$$u_r(r)^{(Thermal)} = r^{-m}(r^{\frac{m-\Phi}{2}}(C_1+C_2r^\Phi)+r\chi) \tag{32a}$$

$$\sigma_r(r)^{(Thermal)} = -\frac{1}{2}\left(\frac{EA}{1-v^2}\right)r^{-1-m-\frac{\Phi}{2}}\begin{pmatrix} C_2r^{\frac{m}{2}+\Phi}(m-2v-\Phi) \\ +C_1r^{m/2}(m-2v+\Phi) \\ +2r^{1+\frac{\Phi}{2}}(-1+m-v)\chi \end{pmatrix} - \frac{E\alpha(r^{-m}\psi_1+\psi_2)}{1-v} \tag{32b}$$

$$\sigma_\theta(r)^{(Thermal)} = \frac{1}{2}\left(\frac{E}{1-v^2}\right)r^{-1-m-\frac{\Phi}{2}}\begin{pmatrix} C_2r^{\frac{m}{2}+\Phi}(2-mv+v\Phi) \\ -C_1r^{m/2}(-2+v(m+\Phi)) \\ -2r^{1+\frac{\Phi}{2}}(-1+(-1+m)v)\chi \end{pmatrix}$$
$$-\frac{E\alpha(r^{-m}\psi_1+\psi_2)}{1-v} \tag{32c}$$

where

$$\psi_1 = \frac{a^m b^m(-T_a+T_b)}{a^m-b^m}, \quad \psi_2 = \frac{a^m T_a - b^m T_b}{a^m-b^m} \tag{33}$$

$$\Delta = -m\alpha(1+v)\psi_1, \quad \chi = \frac{\Delta}{m(-1+v)}, \quad \Phi = \sqrt{4+m^2-4mv}$$

and

$$C_1^{(Free-Free)} = \frac{a^{\frac{\Phi-m}{2}} b^{\frac{\Phi-m}{2}} \left(\begin{array}{c} 2ab^{\frac{m+\Phi}{2}}(\alpha(v+1)(\psi_2 a^m + \psi_1) + \chi(m-v-1)) \\ -2ba^{\frac{m+\Phi}{2}}(\alpha(v+1)(\psi_2 b^m + \psi_1) + \chi(m-v-1)) \end{array} \right)}{(a^\Phi - b^\Phi)(m - 2v + \Phi)}$$

(34a)

$$C_2^{(Free-Free)} = \frac{a^{-m/2} b^{-m/2} \left(\begin{array}{c} 2a^{m/2} b^{\frac{\Phi}{2}+1}(\alpha(v+1)(\psi_2 b^m + \psi_1) + \chi(m-v-1)) \\ -2a^{\frac{\Phi}{2}+1} b^{m/2}(\alpha(v+1)(\psi_2 a^m + \psi_1) + \chi(m-v-1)) \end{array} \right)}{(a^\Phi - b^\Phi)(m - 2v - \Phi)}$$

$$C_1^{(Fixed-Free)} = \frac{a^{\frac{\Phi-m}{2}} b^{\frac{\Phi-m}{2}} \left(\begin{array}{c} a\chi b^{\frac{m+\Phi}{2}}(m - 2v - \Phi) \\ -2ba^{\frac{m+\Phi}{2}}(\alpha(v+1)(\psi_2 b^m + \psi_1) + \chi(m-v-1)) \end{array} \right)}{a^\Phi(m - 2v + \Phi) + b^\Phi(-m + 2v + \Phi)}$$

(34b)

$$C_2^{(Fixed-Free)} = \frac{a^{-m/2} b^{-m/2} \left(\begin{array}{c} 2a^{m/2} b^{\frac{\Phi}{2}+1}(\alpha(v+1)(\psi_2 b^m + \psi_1) + \chi(m-v-1)) \\ -\chi a^{\frac{\Phi}{2}+1} b^{m/2}(m - 2v + \Phi) \end{array} \right)}{a^\Phi(m - 2v + \Phi) + b^\Phi(-m + 2v + \Phi)}$$

$$C_1^{(Fixed-Fixed)} = -\frac{\chi a^\Phi b^{\frac{1}{2}(-m+\Phi+2)} - \chi b^\Phi a^{\frac{1}{2}(-m+\Phi+2)}}{a^\Phi - b^\Phi}$$

(34c)

$$C_2^{(Fixed-Fixed)} = \frac{\chi(b^{\frac{1}{2}(-m+\Phi+2)} - a^{\frac{1}{2}(-m+\Phi+2)})}{a^\Phi - b^\Phi}$$

Elastic fields in a uniform disk due to the thermal loads are obtained as

$$u_r(r)_{(Free-Free/Uniform\ Thickness)}^{(Thermal)} = \frac{\left(\begin{array}{c} a^2(v+1)lna(\vartheta - 2\alpha\Psi_2)\left(\begin{array}{c} b^2(v+1) \\ -(v-1)r^2 \end{array} \right) \\ -b^2(v+1)lnb\left(\begin{array}{c} a^2(v+1) \\ -(v-1)r^2 \end{array} \right)(\vartheta - 2\alpha\Psi_2) \\ +(v-1)r^2(a-b)(a+b)\left(\begin{array}{c} 2\alpha(v+1)\Psi_1 - \vartheta \\ +\vartheta(v+1)lnr \end{array} \right) \end{array} \right)}{2(v-1)(v+1)r(a^2 - b^2)}$$

(35a)

$$\sigma_r(r)_{(Free-Free/Uniform\ Thickness)}^{(Thermal)} = -\frac{E(\vartheta - 2\alpha\Psi_2)\left(\begin{array}{c} b^2(r^2 - a^2)lnb \\ +a^2 lna(b^2 - r^2) \\ +r^2(a^2 - b^2)lnr \end{array} \right)}{2(v-1)r^2(a^2 - b^2)}$$

(35b)

$$\sigma_\theta(r)_{(Free-Free/Uniform\ Thickness)}^{(Thermal)} = \frac{E\left(\begin{array}{c} (v+1)(\vartheta - 2\alpha\Psi_2)\left(\begin{array}{c} a^2 lna(b^2 + r^2) \\ -b^2(a^2 + r^2)lnb \\ +r^2(b^2 - a^2)lnr \end{array} \right) \\ -\vartheta(v-1)r^2(a^2 - b^2) \end{array} \right)}{2(v^2 - 1)r^2(a^2 - b^2)}$$

(35c)

and

$$u_r(r)^{(Thermal)}_{(Fixed-Free/Uniform)} = \frac{\begin{pmatrix} a^2\vartheta lna\begin{pmatrix} b^2(v+1) \\ -(v-1)r^2 \end{pmatrix} - \vartheta r^2 lnr\begin{pmatrix} b^2(v+1) \\ -a^2(v-1) \end{pmatrix} \\ -b^2(a^2-r^2)\begin{pmatrix} -2\alpha(v+1)\Psi_1 \\ +(v+1)lnb(\vartheta-2\alpha\Psi_2)+\vartheta \end{pmatrix} \end{pmatrix}}{2a^2(v-1)r-2b^2(v+1)r} \quad (36a)$$

$\sigma_r(r)^{(Thermal)}_{(Fixed-Free/Uniform\ Thickness)}$

$$= \frac{E\begin{pmatrix} (v+1)(\vartheta-2\alpha\Psi_2)\begin{pmatrix} b^2lnb(a^2(v-1)-(v+1)r^2) \\ +r^2lnr(b^2(v+1)-a^2(v-1)) \end{pmatrix} \\ +a^2(v-1)(b^2-r^2)(\vartheta-2\alpha(v+1)\Psi_1) \\ -a^2\vartheta(v^2-1)lna(b^2-r^2) \end{pmatrix}}{2(v^2-1)r^2(a^2(v-1)-b^2(v+1))} \quad (36b)$$

$\sigma_\theta(r)^{(Thermal)}_{(Fixed-Free/Uniform\ Thickness)}$

$$= \frac{E\begin{pmatrix} a^2(v-1)(2\alpha(v+1)\Psi_1(b^2+r^2)-\vartheta(b^2+vr^2)) \\ +(v+1)(\vartheta-2\alpha\Psi_2)\begin{pmatrix} r^2lnr(b^2(v+1)-a^2(v-1)) \\ -b^2lnb(a^2(v-1)+(v+1)r^2) \end{pmatrix} \\ +a^2\vartheta(v^2-1)lna(b^2+r^2)+b^2\vartheta(v^2-1)r^2 \end{pmatrix}}{2(v^2-1)r^2(a^2(v-1)-b^2(v+1))} \quad (36c)$$

and

$$u_r(r)^{(Thermal)}_{(Fixed-Fixed/Uniform\ Thickness)} = \frac{\vartheta\begin{pmatrix} b^2(r^2-a^2)lnb \\ +a^2lna(b^2-r^2) \\ +r^2(a^2-b^2)lnr \end{pmatrix}}{2r(a^2-b^2)} \quad (37a)$$

$$\sigma_r(r)^{(Thermal)}_{(Fixed-Fixed/Uniform\ Thickness)} = \frac{E\begin{pmatrix} a^2\vartheta lna((v+1)r^2-b^2(v-1)) \\ +b^2\vartheta lnb(a^2(v-1)-(v+1)r^2) \\ -r^2(a^2-b^2)\begin{pmatrix} -2\alpha(v+1)\Psi_1+\vartheta \\ +(v+1)lnr(\vartheta-2\alpha\Psi_2) \end{pmatrix} \end{pmatrix}}{2(v^2-1)r^2(a^2-b^2)} \quad (37b)$$

$$\sigma_\theta(r)^{(Thermal)}_{(Fixed-Fixed/Uniform\ Thickness)} = \frac{E\begin{pmatrix} a^2\vartheta lna(b^2(v-1)+(v+1)r^2) \\ -b^2\vartheta lnb(a^2(v-1)+(v+1)r^2) \\ -r^2(a^2-b^2)\begin{pmatrix} -2\alpha(v+1)\Psi_1+\vartheta v \\ +(v+1)lnr(\vartheta-2\alpha\Psi_2) \end{pmatrix} \end{pmatrix}}{2(v^2-1)r^2(a^2-b^2)} \quad (37c)$$

where

$$\Psi_1 = \frac{T_b lna - T_a lnb}{lna - lnb}, \qquad \Psi_2 = \frac{T_a - T_b}{lna - lnb} \quad (38)$$

$$\vartheta = \alpha(1+v)\Psi_2$$

5. Numerical Examples

A disk made of a stainless steel (SUS304) is chosen with the following properties in numerical examples.

$$a = 0.5 \, m; \; b = 1 \, m; \; \omega = 100 \; (rad/s)$$

$$p_a = 60 \, (MPa); \; p_b = 30 \, (MPa); \; T_b = 100 \, °C; \; T_a = 20 \, °C$$

$$E = 201.04 \, (GPa); \; \rho = 7800 \, (kg/m^3); \; v = 0.3262$$

$$\alpha = 12.33 \; 10^{-6} \, (1/K); \; k = 15.379 \, (W/mK)$$

Dimensionless elastic fields are defined as follows

$$\bar{u}_r(r) = \frac{E}{(1 - v^2)\rho\omega^2 b^3 + (1 + v)\alpha E T_b b + b p_o} u_r(r)$$

$$\bar{\sigma}_r(r) = \frac{(1 - v)}{(1 - v)\rho\omega^2 b^2 + \alpha E T_b + (1 - v)p_o} \sigma_r(r) \tag{39}$$

$$\bar{\sigma}_\theta(r) = \frac{(1 - v)}{(1 - v)\rho\omega^2 b^2 + \alpha E T_b + (1 - v)p_o} \sigma_\theta(r)$$

where $p_o = p_a$ is used for both free-free and fixed-fixed boundary conditions while $p_o = p_b$ for fixed-free surfaces.

As a first example, the radial temperature distribution in a hyperbolic disk is investigated regarding different profile parameters and aspect ratios defined by (a/b). Solutions are illustrated by Fig. 2. As can be seen from Fig. 2 that the differences in the temperature distributions in a hyperbolic disk become much obvious as the aspect ratios get smaller. A convergent disk profile having $m = -1$ exhibits a linear temperature distribution while the other profile parameters offer different curves. The temperatures at the intermediate surfaces of a disk having divergent profiles decrease faster than convergent ones towards the inner surface and increase slowly towards the outer. It is not suitable the use of a linear temperature profile instead of the true one, except $m = -1$, for even uniform disks as seen from Fig. 2.
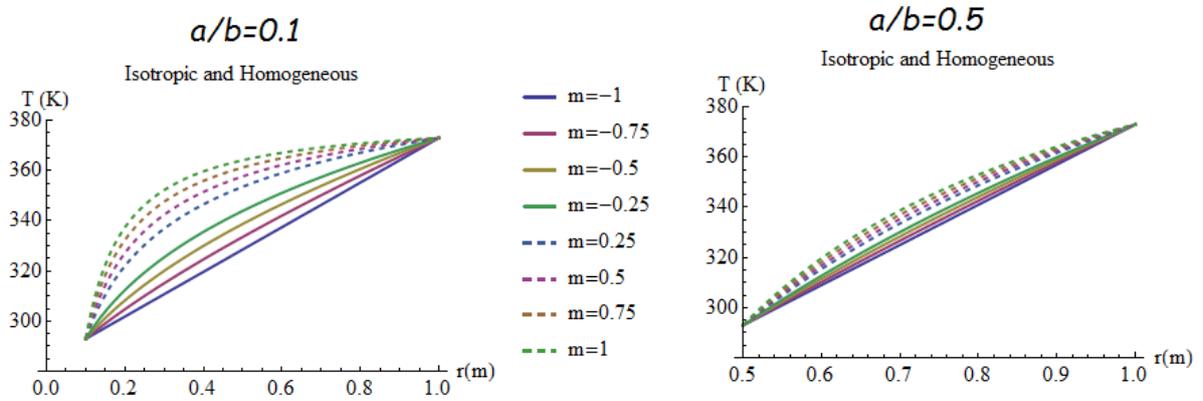

Fig. 2. Variation of the radial temperature distribution with the aspect ratios and profile parameters

As a second example, the radial variations of the elastic fields in a hyperbolic disk with the profile parameters are to be examined. Solutions for three boundary conditions are demonstrated by Fig. 3 in a comparative manner. The numerical values of some equivalent stresses are presented in Table 2.
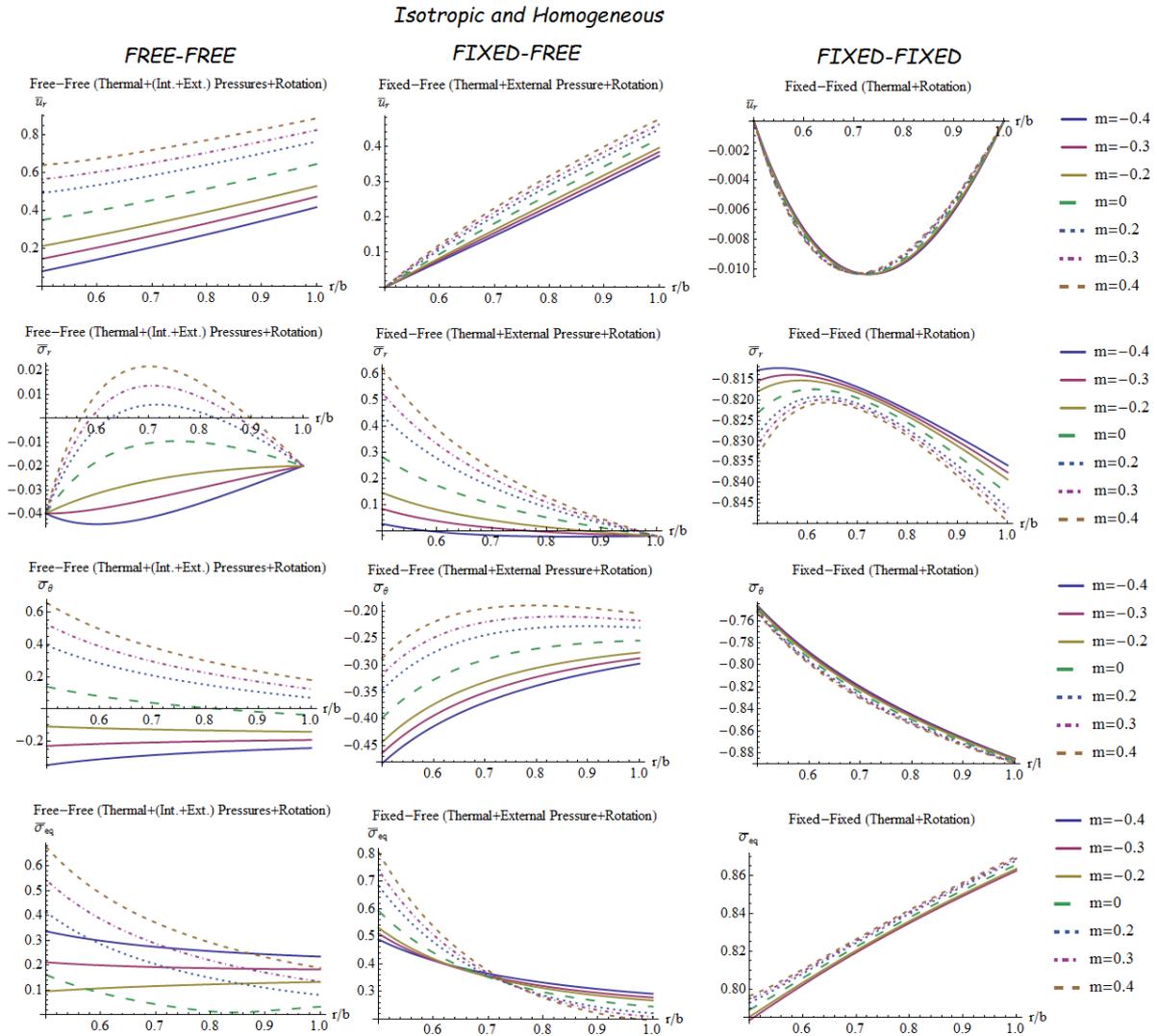

Fig. 3. The radial variations of the elastic fields in a hyperbolic disk with the profile parameters

As can be observed from Fig. 3 that, the curves are in accordance with the related boundary conditions. Observations from this figure are outlined below:

i. The maximum radial displacement is located at the outer surface for free-free and fixed-free boundary conditions while it is in the vicinity of the mid-surface for fixed-fixed hyperbolic disks.

ii. The convergent profiles offer smaller radial displacements than divergent and uniform ones under free-free and fixed-free boundary conditions. The radial displacements in divergent hyperbolic disks are higher than even uniform profiles under free-free and fixed-free boundary conditions.

iii. The radial stress in free-free divergent hyperbolic disks is in compression at the vicinity of both the inner and outer surfaces while it is in tension at the vicinity of mid-surface. However, the radial stresses are all in compression in both uniform and convergent disks under free-free conditions.

iv. The maximum radial stress is at the inner surface under both free-free and fixed-free conditions except for $m = -0.4$ in free-free and fixed-fixed disks.

v. Convergent disk profiles exhibit better response to the radial stress variation than both uniform and divergent ones for fixed-free disks.

vi. Fixed-fixed disks have radial and hoop stresses which are completely in compression. Convergent disk profiles exhibit better response to the combined thermal and centrifugal loads than uniform and divergent ones under fixed-fixed boundary conditions.

vii. When the variation of the hoop stresses are concerned, convergent profiles seem to be better than divergent ones under free-free and fixed-fixed boundaries. The converse is true for fixed-free hyperbolic disks.

viii. For fixed-free disks, divergent profiles having higher parameter values in absolute present better hoop stress distribution.

Table 2. Equivalent stresses in a hyperbolic disk

				m			
	-0.4	-0.3	-0.2	0 $(1.\times 10^{-11})$	0.2	0.3	0.4

Fixed-Fixed (thermal + rotation) $(p_o = p_a)$

	-0.4	-0.3	-0.2	0	0.2	0.3	0.4
0.5	0.916974	0.783478	0.785315	0.788975	0.792691	0.794532	0.796368
0.6	0.980805	0.802161	0.803402	0.805805	0.808167	0.809306	0.810422
0.7	1.02596	0.819335	0.820365	0.822386	0.824401	0.825389	0.826369
0.8	1.06088	0.834924	0.835901	0.83786	0.839837	0.840827	0.84182
0.9	1.08956	0.849215	0.85022	0.852247	0.854303	0.855335	0.856372
1.	1.11416	0.862506	0.86359	0.865748	0.867921	0.868999	0.870072

Fixed-Free (thermal + rotation+ external pressure) $(p_o = p_b)$

	-0.4	-0.3	-0.2	0	0.2	0.3	0.4
0.5	0.489025	0.510427	0.531227	0.593047	0.68397	0.740794	0.805348
0.6	0.412551	0.413534	0.418865	0.440813	0.479528	0.505501	0.535931
0.7	0.364721	0.356252	0.353188	0.35219	0.359343	0.366401	0.375932
0.8	0.332283	0.319776	0.312241	0.298309	0.286529	0.281748	0.277884
0.9	0.309015	0.295211	0.285512	0.265198	0.243728	0.232593	0.221237
1.	0.291673	0.277947	0.267494	0.245311	0.221319	0.208593	0.195358

Free-Free (thermal + rotation+ internal and external pressures) $(p_o = p_a)$

	-0.4	-0.3	-0.2	0	0.2	0.3	0.4
0.5	0.337384	0.212439	0.0952687	0.162293	0.41535	0.545674	0.678143
0.6	0.299193	0.200208	0.10746	0.0890103	0.285386	0.386576	0.48942
0.7	0.274373	0.192891	0.11637	0.0435495	0.204567	0.287646	0.372081
0.8	0.257063	0.188267	0.123151	0.0145655	0.149327	0.219918	0.291667
0.9	0.244496	0.185281	0.128545	0.0161429	0.109388	0.170738	0.233149
1.	0.235186	0.18336	0.133007	0.033027	0.0805358	0.134429	0.189562

ix. For free-free disks, convergent profiles having smaller parameter values in absolute offer better hoop stress variations than divergent ones. For this boundary condition, the uniform disks exhibit the best response to the circumferential stresses together with $m = -0.2$.

x. As to the equivalent von-Misses stresses, fixed-free and fixed-fixed boundaries need convergent disks having higher parameter values in absolute while free-free disks require convergent disk having smaller parameter values.

xi. Convergent profiles may exhibit almost uniform equivalent stresses under free-free boundary conditions. According to Fig. 3, $m = -0.2$ is the best for the distribution of equivalent von-Misses stresses under free-free conditions.

6. Conclusions

Closed-form formulas were proposed for hyperbolic disks made of traditional materials under free-free, fixed-free, and fixed-fixed boundary conditions to obtain the exact thermo-mechanical fields. Combined thermal loads, internal and external pressures, and centrifugal forces were considered as thermo-mechanical loads. Those formulas are to be very helpful tools in the pre-design stage of such disks.

To the best of the author's knowledge, formulas for the hyperbolic fixed-free disks subjected to the external pressure induced by the existence of the blades have been originally offered in the present study.

References

[1] Güven, U., Altay O., Elastic–plastic solid disk with nonuniform heat source subjected to external pressure, Int J Mech Sci, 42(5), 831-842, 2000.

[2] Jahed, H., Shirazi, R., Loading and unloading behaviour of a thermoplastic disc, Int. J Pressure Vessels Piping, 78, 637–645, 2001.

[3] Gogulwar, V.S., Deshmukh, K.C., An inverse quasi-static thermal stresses in an annular disc, Proceeding of ICADS, Narosa Publishing House, New Delhi, 2002.

[4] Kulkarni, V.S., Deshmukh, K.C., Thermal stresses in a thick annular disc, Journal of Thermal Stresses, 31(4), 331-342, 2008.

[5] Genç, M.S., Özşik, G., Yapıcı, H., A numerical study of the thermally induced stress distribution in a rotating hollow disc heated by a moving heat source acting on one of the side surfaces, P I Mech Eng C-J Mec, 223(8), 1877-1887, 2009.

[6] Nejad, M.Z., Afshin, A., Transient thermoelastic analysis of pressurized rotating disks subjected to arbitrary boundary and initial conditions, Chinese Journal of Engineering, Article ID 894902, 13 pages, 2014. http://dx.doi.org/10.1155/2014/894902

[7] Rattan, M., Kaushik, A., Chamoli, N., Steady state creep behavior of thermally graded isotropic rotating disc of composite taking into account the thermal residual stress, European Journal of Mechanics A/Solids, 60, 315-326, 2016.

[8] Kaur, J., Thakur, P., Singh, S.B., Steady thermal stresses in a thin rotating disc of finitesimal deformation with mechanical load, Journal of Solid Mechanics, 8(1), 204-211, 2016.

[9] Nayak, P., Saha, K., Elastic limit angular speed of solid and annular disks under thermomechanical loading, International Journal of Engineering, Science and Technology, 8(2), 30-45, 2016.

[10] Yıldırım, V., Heat-induced, pressure-induced and centrifugal-force-induced exact axisymmetric thermo-mechanical analyses in a thick-walled spherical vessel, an infinite

cylindrical vessel, and a uniform disc made of an isotropic and homogeneous material, Int J Eng Appl Sci (IJEAS), 9(2), 66-87, 2017. Doi: 10.24107/ijeas.309786.

[11] Sayman, O. Thermal stress analysis in an aluminum metal-matrix orthotropic disc, Journal of Reinforced Plastics and Composites, 23, 1473-1479, 2004.

[12] Çallıoğlu, H., Topçu, M., Altan, G., Stress analysis of curvilinearly orthotropic rotating discs under mechanical and thermal loading, Journal of Reinforced Plastics and Composites, 24(8), 831-838, 2005.

[13] Çallıoğlu, H., Thermal stress analysis of curvilinear orthotropic rotating disks, Journal of Thermoplastic Composite Materials, 20, 357-369, 2007.

[14] Sen, F., Sayer, M., Elasto-plastic thermal stress analysis in a thermoplastic composite disc under uniform temperature using FEM, Mathematical and Computational Applications, 11(1), 31-39, 2006.

[15] Altan, G., Topçu, M., Bektaş, N.B., Altan, B.D., Elastic-plastic thermal stress analysis of an aluminum composite disc under parabolic thermal load distribution, J. Mech. Sci. Technol., 22(12), 2318–2327, 2008.

[16] Mohammadi, F., Hadadian, A., Singh, G.J., Analytical solution of pressurized rotating composite disk under thermal loading, Proceedings of the World Congress on Engineering II: WCE 2010, London, U.K. (4 pages) 2010.

[17] Mustafa, M.T., Zubair, S.M., Arif, A.F.M., Thermal analysis of orthotropic annular fins with contact resistance: A closed-form analytical solution, Appl. Therm. Eng., 31, 937–945, 2011.

[18] Kansal, G., Parvez, M., Thermal stress analysis of orthotropic graded rotating discs, International Journal of Modern Engineering Research (IJMER), 2(5), 3381-3885, 2012.

[19] Stampouloglou, I.H., Theotokoglou, E.E., The radially nonhomogeneous thermoelastic axisymmetric problem, Int J Mech Sci, 120, 311–321, 2017.

[20] Bayat, M., Saleem, M., Sahari, B.B., Hamouda, A.M.S., Mahdi, E., Thermo elastic analysis of a functionally graded rotating disk with small and large deflections, Thin-Wall Struct, 45, 677–691, 2007.

[21] Kordkheili, S.A.H., Naghdabadi, R., Thermoelastic analysis of a functionally graded rotating disk, Compos Struct, 79, 508–516, 2007.

[22] Arani, A.G., Mozdianfard, M.R., Maraghi, Z.K., Shajari, A.R., Thermo-piezo-magneto-mechanical stresses analysis of FGPM hollow rotating thin disk, Int J Mech Mater Des, 6, 341–349, 2010.

[23] Afsar, A.M., Go, J., Finite element analysis of thermoelastic feld in a rotating FGM circular disk, Appl. Math. Model, 34, 3309–3320, 2010.

[24] Peng, X.L., Li, X.F., Thermal stress in rotating functionally graded hollow circular discs, Compos Struct, 92(8), 1896–1904, 2010.

[25] Kursun, A., Topçu, M., Tetik, T., Stress analysis of functionally graded disc under thermal and mechanical loads, ICM11, Engineering Procedia, 10, 2949–2954, 2011.

[26] Gong, J.F., Ming, P.J., Xuan, L.K., Zhang, W.P., Thermoelastic analysis of three-dimensional functionally graded rotating disks based on finite volume method, P I Mech Eng C-J Mec, 228(4), 583–598, 2014.

[27] Gonczi, D., Ecsedi, I., Thermoelasic analysis of functionally graded hollow circular disk, Arch Mech Eng, LXII, 5–18, 2015.

[28] Yıldırım, V., Thermomechanical characteristics of a functionally graded mounted uniform disc with/without rigid casing, The Journal of Aerospace Technology and Management (JATM), 2018. (to be published)

[29] Chiba, R., Stochastic thermal stresses in an FGM annular disc of variable thickness with spatially random heat transfer coefficients, Meccanica, 44, 159–176, 2009.

[30] Bayat, M., Saleem, M., Sahari, B.B., Hamouda ,A.M.S, Mahdi E., Mechanical and thermal stresses in a functionally graded rotating disk with variable thickness due to radially symmetry loads, Int. J Pressure Vessels Piping, 86, 357–372, 2009.

[31] Bayat, M., Sahari, B.B., Saleem, M., Ali, A., Wong, S.V., Thermoelastic solution of a functionally graded variable thickness rotating disk with bending based on the first-order shear deformation theory, Thin-Wall Struct, 47, 568–582, 2009.

[32] Bayat, M., Sahari, B.B., Saleem, M., Hamouda, A.M.S., Reddy, J.N., Thermo elastic analysis of functionally graded rotating disks with temperature-dependent material properties: uniform and variable thickness, Journal of Mechanics and Materials in Design, 5(3), 263–279, 2009.

[33] Bayat, M., Mohazzab, A.H., Sahari, B.B., Saleem, M., Exact solution for functionally graded variable-thickness rotating disc with heat source, P I Mech Eng C-J Mec, 224(11), 2316–2331, 2010.

[34] Arani, G., Loghman, A., Shajari, A., Amir, S.A.R., Semi-analytical solution of magneto-thermo-elastic stresses for functionally graded variable thickness rotating disks, J Mech Sci Technol, 24(10), 2107–2117, 2010.

[35] Nie, G.J., Batra, R.C., Stress analysis and material tailoring in isotropic linear thermoelastic incompressible functionally graded rotating disks of variable thickness, Compos Struct, 92, 720–729, 2010.

[36] Damircheli, M., Azadi, M., Temperature and thickness effects on thermal and mechanical stresses of rotating FG-disks, J Mech Sci Technol, 25(3), 827-836, 2011.

[37] Hassani, A., Hojjati, M.H., Farrahi, G., Alashti, R.A., Semi-exact elastic solutions for thermo-mechanical analysis of functionally graded rotating disks, Compos Struct, 93(12), 3239–3251, 2011.

[38] Tutuncu, N., Temel, B., An efficient unified method for thermoelastic analysis of functionally graded rotating disks of variable thickness, Mechanics of Advanced Materials and Structures, 20(1), 38-46, 2013.

[39] Golmakani, M.E., Large deflection thermoelastic analysis of shear deformable functionally graded variable thickness rotating disk, Composites: Part B, 45, 1143-1155, 2013.

[40] Kurşun, A., Topçu, M., Thermal stress analysis of functionally graded disc with variable thickness due to linearly increasing temperature load, Arab J Sci Eng, 38, 3531–3549, 2013.

[41] Mahdavi, E., AkbariAlashti, R., Darabi, A.C., Alizadeh, M., Linear thermoplastic analysis of FGM rotating discs with variable thickness, Iranian Journal of Mechanical Engineering, 14(2), 73-87, 2013.

[42] Jabbari, M., Ghannad, M., Nejad, M.Z., Effect of thickness profile and FG function on rotating disks under thermal and mechanical loading, Journal of Mechanics, 32(1), 35-46, 2016.

[43] Vivio, F., Vullo, V., Elastic stress analysis of rotating converging conical disks subjected to thermal load and having variable density along the radius, Int J Solids Struct, 44, 7767–7784, 2007.

[44] Vullo, V., Vivio, F., Elastic stress analysis of non-linear variable thickness rotating disks subjected to thermal load and having variable density along the radius, Int J Solids Struct, 45, 5337–5355, 2008.

[45] Garg, M., Salaria, B.S., Gupta, V.K., Effect of thermal gradient on steady state creep in a rotating disc of variable thickness, Procedia Eng., 55, 542e547. 2013.

[46] Çetin, E., Kurşun, A., Aksoy, Ş., Çetin, M.T., Elastic stress analysis of annular bi-material discs with variable thickness under mechanical and thermomechanical loads, World Academy of Science, Engineering and Technology, International Journal of Mechanical, Aerospace, Industrial, Mechatronic and Manufacturing Engineering, 8(2), 288-292, 2014.

[47] Zwillinger, D. Handbook of Differential Equations, 3rd ed. Boston, MA: Academic Press, p. 120, 1997.

[48] Yıldırım, V., Effects of inhomogeneity and thickness parameters on the elastic response of a pressurized hyperbolic annulus/disc made of functionally graded material, Int J Eng Appl Sci, 9(3), 2017. Doi: 10.24107/ijeas.329433

[49] Young, W.C., Budynas, R.G., Roark's Formulas for Stress and Strain; McGraw Hill, Seventh Edition, New York. 2002.

[50] Yıldırım, V., Analytic solutions to power-law graded hyperbolic rotating discs subjected to different boundary conditions, International Journal of Engineering & Applied Sciences (IJEAS), 8(1), 38-52, 2016.

[51] Yıldırım V., A parametric study on the centrifugal force-induced stress and displacements in power-law graded hyperbolic discs, Latin American Journal of Solids and Structures, LAJSS, 15(4) e34, 1-16, 2018. Doi: 10.1590/1679-78254229